

Undergraduate Research on Adding Relay Models and Generator Capability Curves to Synthetic Electric Grids

Stephen E. Hurt, Jonathan Snodgrass, Thomas J. Overbye

Department of Electrical and Computer Engineering

Texas A&M University

College Station, TX

{stephenhurt99; snodgrass; overbye;}@tamu.edu

Abstract—Synthetic electric power systems are important models that allow researchers to conduct and publish their work without using nonpublic data about the real grid. These synthetic grids are often missing models that are important to certain studies, such as, fault analysis, cascading failure, or geomagnetically induced currents (GICs). Furthermore, these cases often lack the data to build these models because the data is nonpublic, or the data is synthetic. Because the data is synthetic, it is generally within an acceptable range, but it might not necessarily be precise enough for certain models such as generator capability curves. Using the synthetic data to build the generator capability curves, will often lead to unrealistic results. The generator capability curves can instead be estimated using data from the existing data set. Line distance relay and time-overcurrent relay models can also be added to the case, using known data. With these models, a synthetic case can be made much more realistic without the need to obtain or protect nonpublic, real grid data.

Index Terms—Power Systems, Synthetic Networks, Line Distance Relay, Time-Overcurrent Relay, Generator Capability Curve

I. INTRODUCTION

Synthetic electric grids provide valuable models that mimic the grid, but contain no nonpublic information about the real grid. They are important to the community of power and energy researchers because, in their absence, the results of important and globally relevant studies cannot be published or shared with others [1], [2]. It is important that a synthetic grid contain the necessary components that should be modeled for a given research project. For instance, geomagnetic disturbances (GMDs) and electromagnetic pulses (EMPs) cause reactive power losses because the GICs saturate the transformers which can ultimately lead to voltage collapse [3], [4].

Generator capability curves are an accurate model of a generator's reactive power capability. A generator's reactive power capability is limited by its armature current limit, field current limit, and end-region heating limit [5]. According to

the North American Electric Reliability Commission (NERC), loss of reactive power support is a key risk to the electric grid caused by GICs [6]. Because reactive power losses are a key risk to the electric grid when GICs are present, it is important to model each generator's reactive power capability more accurately. There are well known methods for calculating generator capability curves. Accurate methods for creating these curves is shown in [5], [7]–[10]. The problem with these methods, is that they rely on a few specific generator parameters such as the synchronous reactance X_s or the short circuit ratio (SCR). In synthetic cases, these parameters, which are stored in the case, are synthetic and often produce unrealistic generator capability curves when used as they are described in the listed sources. For this reason, they do not provide a helpful algorithm to create synthetic generator capability curves. A novel method to create these curves is formulated in [11], but this method assumes a minimum lagging power factor of 0.8, and a minimum leading power factor of 0.95. These assumptions, although common and reasonable, may not make sense when minimum reactive power is at a power factor greater than 0.95. This paper presents a novel algorithm for creating generator capability curves.

Line relays are another important component of a synthetic case that can be difficult and time consuming to add to a model. They are important because they have the potential to dramatically affect the solution of a transient stability run. For instance, in a transient stability study that includes GIC flows, it is important to include relays because the added current caused by the GIC flows could be enough to open a relay which would not be detected if there are no relays in the case. Relays have the potential to cause cascading failure especially on a heavily loaded system. Without relays in a case, a transient stability run with a given contingency might converge when, in reality, it would have caused a blackout because the contingency caused other lines to overload, which led to cascading failure [12]. For these reasons, it is sometimes necessary to add these models to a synthetic case so that it will provide results that are reasonably similar to the real grid. This can become a cumbersome and monotonous task when it must be done for large cases. The authors did not find any existing

methods for automating relay settings. Typically relays are added one or a handful at a time, and thus there has been no need for automation. However, with recent changes to the power system such as bidirectional power flows on lines that were typically unidirectional or fault currents being limited by inverter-based generation, large-scale reevaluation and recalculation of relay settings might become commonplace. This paper will show how to quickly create synthetic relay models and synthetic generator capability curves.

This paper is organized into the following sections. Section II discusses the development of synthetic relay models. Section III demonstrates an algorithm to create synthetic generator capability curves. Finally, Section IV concludes the paper with a discussion of the results, and potential future work.

II. DEVELOPING SYNTHETIC RELAY MODELS

Relays are an important aspect of a synthetic case because they make a given case behave more like the real grid. When a transient stability is run for a given contingency, for instance a fault, it may cause the case to black out or fail to converge when, in reality, a relay would have opened and only a single line would have lost power. On the other hand, a transient stability run might converge, but on closer examination, it is easily determined that many relays would have opened on the real grid under such conditions. This section will show how to quickly add line distance relay and overcurrent relay models to a synthetic case with typical values. The relay creation techniques are demonstrated using a 2000 bus synthetic Texas electric grid, available at [13] that covers the approximate geographic footprint of the Texas ERCOT system [1], [14]. Since it represents a typical 115 kV transmission line, circuit 1 of the 138 kV transmission line between buses 1001 and 1064 is used to demonstrate the effectiveness of the proposed techniques.

A. Line Distance Relays

Line distance relays protect lines by reading the current and voltage on a branch and using these to compute the impedance of the line and load connected to it. When the impedance of the line enters a set region, the relay considers it a fault [15]. The implementation becomes more complicated when multiple lines are considered. The relay should only trip when the fault is on the line that the relay protects. If the fault is on the next line, the distance relay will still detect the change in impedance. Because of this, time delays are introduced so that the relay nearest the fault will trip before the relays farther from the fault. These time delays also provide backup protection if a relay fails to open. These time delays for different impedance ranges are typically separated into three zones [15], [16]. Figure 1 is a schematic of these three zones with their respective time delays.

The time vs. impedance graph in Figure 1 shows the time delays for relay 1. Zone 1 is typically set to protect close to 90% of the line length, zone 2 is typically set to protect 100% of the line plus 50% of the shortest connected line, and zone

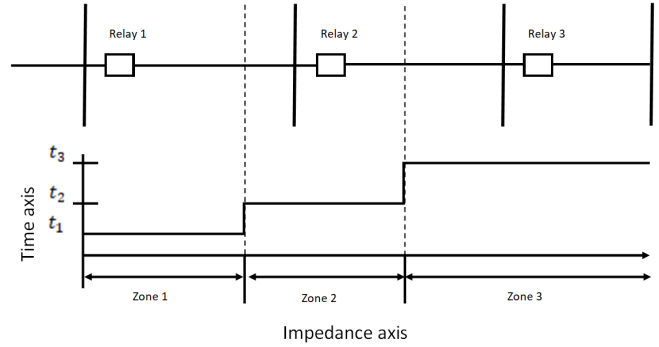


Fig. 1. Time vs. Impedance Zone Schematic for a Simple Distance Relay.

3 is typically set to protect 100% of two lines plus 25% of the third line [17].

This study does not attempt to implement the full complexity of line distance relays, but instead, it proposes a method to quickly (on the order of 5 seconds), add these important models to a synthetic case. An algorithm for creating these models that depends on the other lines connected to the bus is beyond the scope of this paper and is left for future work. To simplify the process, and still provide adequate line protection, the lines are all treated as having the same total impedance. Zone 1 protection was chosen to be 90% of the line, zone 2 was chosen to be 120% of the line, and zone 3 was chosen to be 220% of the line. This simplification will lead to over-reach of zones 2 and 3 where the relay is setup on a long line that is connected to a bus where much shorter lines are connected. Conversely, zones 2 and 3 will under-reach, if the relay is setup on a short branch that connects to much longer branches. This is an acceptable consequence because zones 2 and 3 only exist to provide backup protection if the relays fail on the connecting lines. This means that breaker and relay failure will not be modeled which is acceptable for most non-system protection studies that should incorporate relays. This is because contingencies modeling breaker failure are typically provided by a RTO or utility's system protection group, and tools for creating these contingency lists already exist.

Typical line distance relay models can be easily and quickly created with data stored in the synthetic case. The impedance angle and magnitude of the line to be protected was found in the case. The impedance angle of the line was used for the impedance angle of the protection zone for all three zones. 90% of the impedance magnitude of the line was used for zone 1, 120% of the impedance magnitude was used for zone 2, and 220% of the impedance magnitude was used for zone 3. The time delay for zone 1 is set to be 1 cycle of the system frequency (60Hz for the United States), the time delay for zone 2 is set to be 0.1 seconds, and the time delay for zone 3 is set to be 0.5 seconds. The relays were set to re-close once after 10 cycles, and then remain open if there is still a fault present. Load blinders, which prevent the relay from tripping when the impedance of the load begins to enter one of the protection zones, were not attempted in this study. Synthetic

load blinders are a topic for future work. Figure 2 shows the protection zones for a branch with these values.

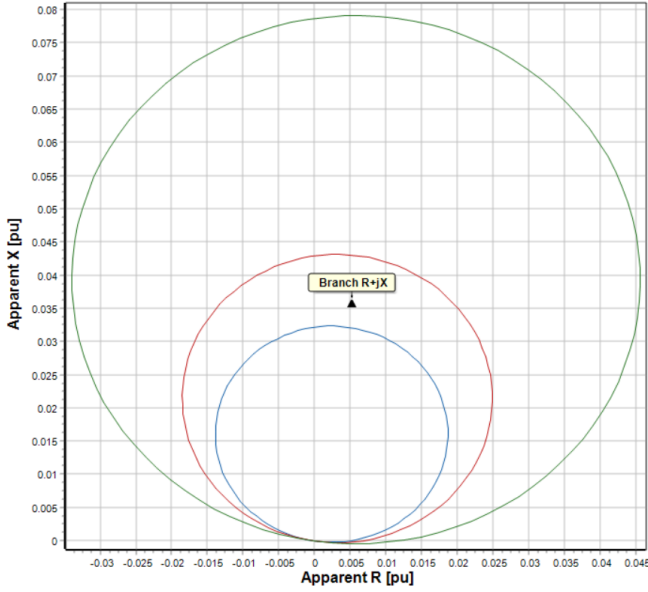


Fig. 2. Typical Relay Zones: Branch 1001-1064 Circuit 1 in the Texas 2000 Bus Case

In Figure 2, the blue circle covers zone 1, the red circle covers zone 2, and the green circle covers zone 3. The Black triangle is the line impedance.

Without any relays in the 2000 bus case, a balanced three phase fault at 50% of the line was applied to an example 115kV transmission line in the 2000 bus case (circuit 1 of the branch between buses 1001 and 1064). Figure 3, shows the current with respect to time in the branch with the fault and in the branch parallel to it.

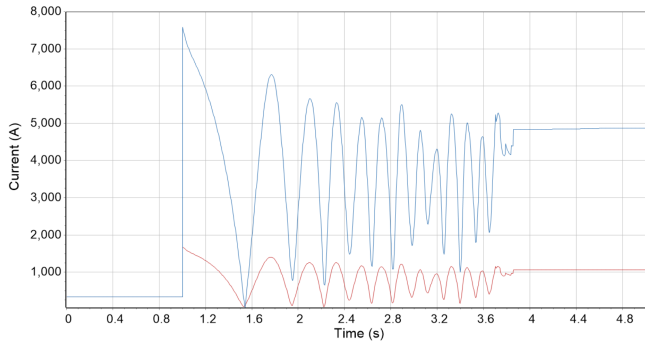


Fig. 3. Current in Branch 1001-1064 Circuits 1 and 2: Texas 2000 Bus Case with No Relays

In Figure 3, the blue line is branch 1001-1064 circuit 1 which had the balanced three phase fault applied at 50% of the branch, and the red line is branch 1001-1064 circuit 2 which is in parallel with the branch with the fault.

After the relays were placed at both ends of every branch in the case with the parameters previously listed, a transient stability study was run with a balanced three phase fault at

0%, 50%, and 100% of the line on branch 1001-1064 circuit 1 in the Texas 2000 bus case [1]. Each graph was very similar, so only the fault at 50% of the line is presented in Figure 4. In Figure 4, the fault current is graphed with respect to time.

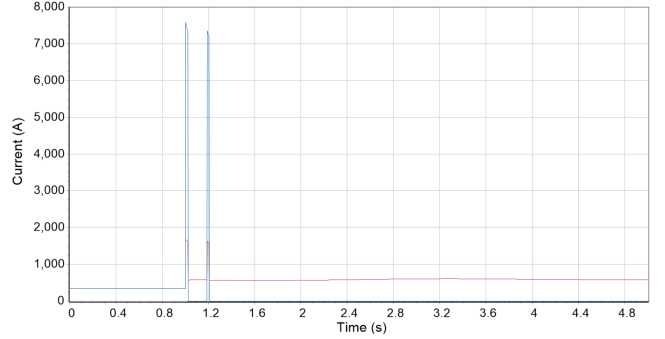


Fig. 4. Current in Branch 1001-1064 Circuits 1 and 2: Texas 2000 Bus Case with Line Distance Relays

In Figure 4, the blue line is the current in the branch with the fault, and the red line is the current in the branch that is in parallel with the branch with the fault. From these two graphs, it is easy to see that the relays are behaving as they were designed. In Figure 3, for the case with no relays, the currents in the two branches spike, and then eventually stabilize with far more current than they can handle. In Figure 4, for the case that has relays, the currents spike, and then the relay opens only the branch with the fault, it stays open for 10 cycles and then re-closes on the fault, it then re-opens and remains open. Circuit 2, which is in parallel with the branch with the fault, then carries more current because the current is no longer distributed between both circuits. A simulation under fault conditions was run to show that the relays operated correctly. The goal of including these models, however, is to use them in studies that do not include faults, such as GMD or EMP studies.

B. Time-Overcurrent Relays

The time-overcurrent relay is one of the oldest relays, but it is still in use today [15]. The time-overcurrent relay is modeled by a straightforward equation with several constants that can be manipulated for the purpose of achieving relay coordination. (1) from [17], [18], is the time-overcurrent relay equation.

$$t_{pickup} = TD \left(\frac{A}{\left(\frac{I}{I_{thresh}} \right)^p - 1} + B \right) \quad (1)$$

In (1), t_{pickup} is the time delay until the relay opens, I is the current in the branch, I_{thresh} is the threshold current, and p , TD , A , and B are parameters that can be manipulated to achieve relay coordination. From [17], [18], 2.0 is a typical value for p that causes a rapid decay in the time-overcurrent curve. To create the synthetic models, t_{pickup} was set at 0.1 seconds when the current is twice I_{thresh} , and I_{thresh} was set to be 110% of the line limit to prevent tripping at

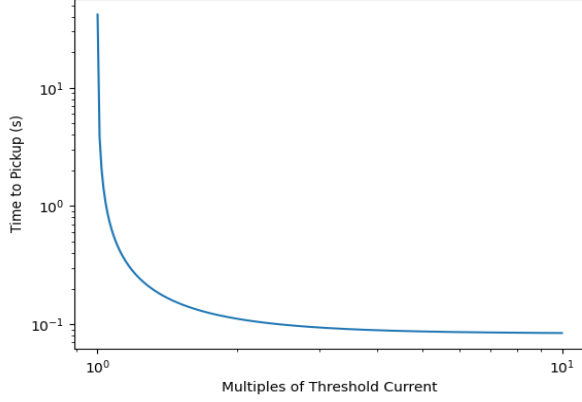


Fig. 5. Typical Time-Overcurrent Curve: Branch 1001-1064 Circuit 1 in Texas 2000 Bus Case

peak load times. TD was set at 1, and $A = B$. To achieve relay coordination, these choices might be incorrect, but relay coordination is not attempted in this study. This is enough information to solve (1) for A and B . The model for the time-overcurrent relays then becomes (2).

$$t_{pickup} = \frac{0.0833}{\left(\frac{I}{I_{thresh}}\right)^2 - 1} + 0.0833 \quad (2)$$

Setting t_{pickup} to 0.1 seconds when the current is twice I_{thresh} is not a random choice. In the line distance relays that were designed previously, 0.1 seconds is the delay for zone 2. Using these values, it is intended that the time-overcurrent relays be used as backup relays with the line distance relays. This will give the line distance relays time to open for zone 1, and provide backup with zones 2 and 3. The time-overcurrent curve for this relay model is shown in Figure 5.

With this relay model implemented at both ends of every branch in the Texas 2000 bus case, a balanced three phase fault was simulated at 0%, 50%, and 100% of the line at branch 1001-1064 circuit 1. The breaker opened as it was designed in all three cases. Figure 6 shows the currents in the branch with the fault and in circuit 2 which is in parallel with the branch with the fault.

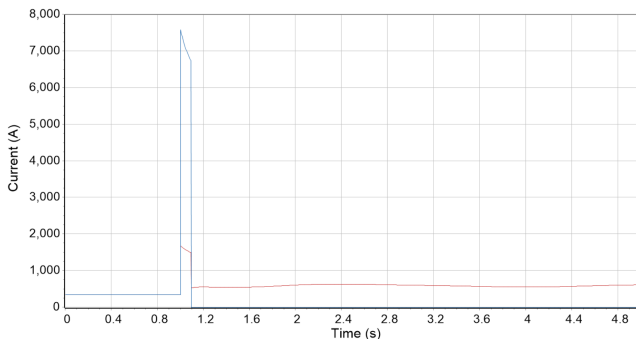


Fig. 6. Current in Branch 1001-1064 Circuits 1 and 2: Texas 2000 Bus Case with Time-Overcurrent Relays

In Figure 6, the blue line is the current in branch 1001-1064 circuit 1 which had the fault applied to it. The red line is the current in branch 1001-1064 circuit 2 which is in parallel with the branch with the fault. From Figure 6, it is clear that the time-overcurrent relay opened without opening the line in parallel with it.

Line distance relay and time-overcurrent relay models can be quickly and easily added to synthetic cases with existing data sets using this algorithm. For the 2000 bus case, a python script (version 3.9) was written to create both types of relays. This script interacts with PowerWorld and takes advantage of the EasySimAuto python package. This script shows that this algorithm is straightforward enough to automate which makes it easy to improve synthetic cases.

III. CREATING GENERATOR CAPABILITY CURVES

A synthetic generator capability curve can be formulated by making three assumptions.

- 1) The capability curve is the intersection of three circles.
- 2) The minimum and maximum real and reactive power limits that are given create a rectangular capability “box” that fits completely within the actual generator capability curve.
- 3) The maximum rated apparent power output is greater than the maximum apparent power output as calculated from the maximum real and reactive power output as defined in the synthetic case.

The three circles that make up the generator capability curve are the armature current limit, the field current limit, and the end-region heating limit.

A. Armature Current Limit

The armature current limit [5] can be modeled by (3), where P is the real power output, Q is the reactive power output, and S_{max} is the maximum apparent power output calculated from (4) below. In (4), P_{max} and Q_{max} are the maximum real and reactive power defined in the synthetic case.

$$P^2 + Q^2 \leq S_{max}^2 \quad (3)$$

$$P_{max}^2 + Q_{max}^2 = S_{max}^2 \quad (4)$$

B. Field Current Limit

The field current limit is modeled by a circle with a center on the Q -axis below the P -axis. Three equations are used to find the field current limit. (5a) is the circle that models the field current limit [11]. (5b) finds the center of that circle. Finally, (5c) finds the radius of that circle [11].

$$P^2 + (Q - Q_{0,field})^2 \leq r_{field}^2 \quad (5a)$$

$$Q_{0,field} = \frac{Q_{max,a}^2 - S_{max}^2}{2\left(Q_{max,a} - S_{max}\sqrt{1 - pf_{lagging}^2}\right)} \quad (5b)$$

$$r_{field} = Q_{max,a} - Q_{0,field} \quad (5c)$$

In the above three equations, $Q_{0,field}$ is the center of the circle, r_{field} is the radius of the circle, P is the real power

output of the generator, Q is the reactive power output of the generator, S_{max} is the maximum apparent power output as calculated in (4), $Q_{max,a}$ is the maximum reactive power as calculated in (6a), and finally, $pf_{lagging}$ is the minimum power factor as calculated from (6b).

$$Q_{max,a} = \sqrt{S_{rated}^2 - P_{max}^2} \quad (6a)$$

$$pf_{lagging} = \frac{P_{max}}{S_{max}} \quad (6b)$$

In the previous two equations, S_{rated} is the maximum rated apparent power output of the generator, and the other variables are the same as defined previously. The maximum rated apparent power output of the generator was chosen because (5b) is found using trigonometry. In this trigonometric problem there is not enough information to solve it without knowing $Q_{max,a}$. It is known that $Q_{max,a}$ should be larger than Q_{max} . The maximum rated apparent power is larger than the maximum apparent power calculated in (4) which means (6a) will give us a reasonable value for $Q_{max,a}$. From [5], (7) below is the actual center of the circle.

$$Q_{0,field} = -\frac{V_t^2}{X_s} \quad (7)$$

In (7), V_t is the armature terminal voltage and X_s is the synchronous reactance. For synthetic cases, (7) will often yield unrealistic results because the generator parameters are synthetic. As such, they are not necessarily related to the generator capability curve in the way that they should be. For this reason, it is preferred to use (5b) to obtain a realistic value for $Q_{0,field}$.

C. End-Region Heating Limit

The end-region heating limit is modeled by a circle with a center on the Q -axis above the P -axis. Three equations are used to find the end-region heating limit. (8a) is the circle that models the end-region heating limit [11]. (8b) finds the center of that circle. Finally, (8c) finds the radius of that circle [11].

$$P^2 + (Q - Q_{0,end})^2 \leq r_{end}^2 \quad (8a)$$

$$Q_{0,end} = \frac{Q_{min,a}^2 - S_{max}^2}{2 \left(Q_{min,a} + S_{max} \sqrt{1 - pf_{leading}^2} \right)} \quad (8b)$$

$$r_{end} = Q_{0,end} - Q_{min,a} \quad (8c)$$

In the three equations above, $Q_{0,end}$ is the center of the circle that lies on the Q -axis, r_{end} is the radius of the circle, $Q_{min,a}$ is the actual minimum reactive power output as determined by (9a), and $pf_{leading}$ is the minimum power factor as determined by (9b).

$$Q_{min,a} = \sqrt{S_{rated}^2 - pf_{leading}^2 S_{max}^2} \quad (9a)$$

$$pf_{leading} = \frac{P_{max}}{\sqrt{P_{max}^2 + Q_{min}^2}} \quad (9b)$$

The previous definitions of the parameters in the above two equations apply. The center of the circle that sweeps out the arc that models the end-region heating limit, $Q_{0,end}$, was found using trigonometry. As with the field current limit, there is not enough information to solve the trigonometry problem without knowing $Q_{min,a}$. (9a) produces a reasonable value for $Q_{min,a}$ by the same reasoning that (6a) produces a reasonable value for $Q_{max,a}$. (10) below is the actual center of the circle [8].

$$Q_{0,end} = \frac{SCR}{2} + \frac{1}{2X_e} \quad (10)$$

In (10), SCR is the short circuit ratio, and X_e is the external reactance [8]. For the same reason (7) could not be used to determine the center of the field current limit circle, (10) cannot be used. In synthetic cases, specific generator parameters are also synthetic. Thus, they do not necessarily relate to the generator capability curve in the way that they should. Using (10) will often yield unrealistic generator capability curves because of this problem.

D. Results

Within the stated assumptions, this algorithm produces reasonable results. Figure 7 is a typical generator capability curve produced by this algorithm.

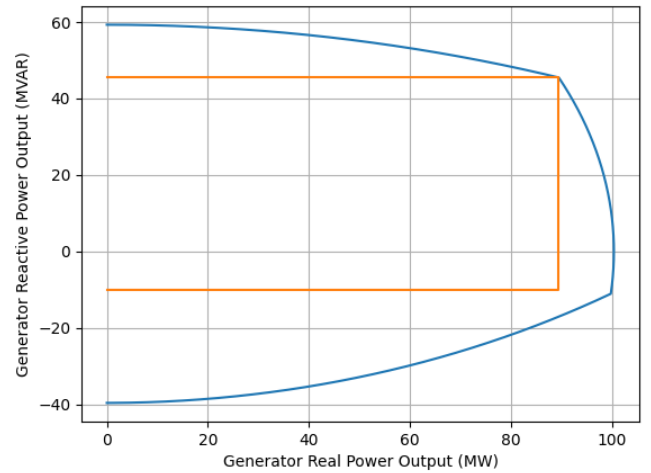


Fig. 7. Synthetic Generator Capability Curve for the Generator at Bus 1050.

In Figure 7, the orange line is the capability "box" from assumption 2, and the blue line is the synthetic generator capability curve produced by this algorithm. Notice in Figure 7 that the bottom right corner of the original capability "box" does not intersect the synthetic generator capability curve. This model can easily be formulated such that it does, by replacing S_{max} with P_{max} in (8b). This is not a simple substitution, but deriving (8b) again with this criterion yields that result. This is undesirable for this model because it also means that every generator capability curve produced with that model has zero negative reactive power capability at its maximum apparent power output. In other words, the end-region heating limit intersects the P -axis. This result is less typical. As such, S_{max}

was used to generate a reasonably accurate synthetic generator capability curve. Figure 8 shows the result of using P_{max} in place of S_{max} in (8b). In Figure 8, the orange line is the generator capability "box," and the blue line is the generator capability curve produced by using P_{max} instead of S_{max} in (8b).

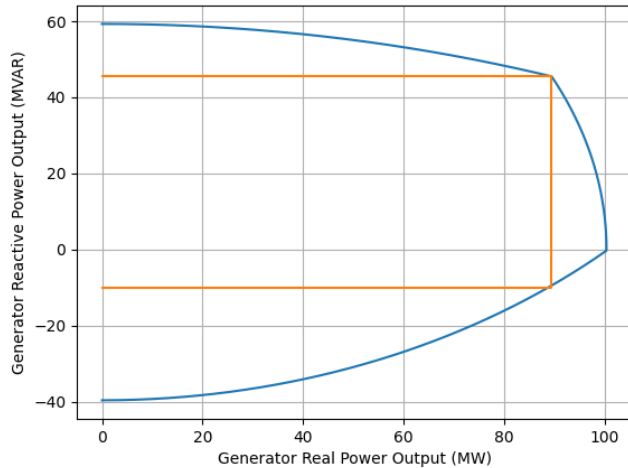


Fig. 8. Alternate Synthetic Generator Capability Curve for the Generator at Bus 1050.

This algorithm successfully produces typical generator capability curves within the stated assumptions. A python script was written to build a synthetic generator capability curve for every generator in the 2000 bus case except wind and solar generators. This shows that this algorithm allows generator capability curves to be quickly and efficiently added to synthetic cases.

IV. CONCLUSION

For certain studies, it is sometimes necessary to add relay models and generator capability curves to a synthetic case which can be time consuming, or require unknown data. With the presented algorithms, these models can be quickly added to a synthetic case with data that is already known and stored in the case.

For the line distance relays, the model is accurate enough to be used in dynamic simulations, but zones 2 and 3 could overreach or under-reach in many cases. This is an acceptable consequence because backup protection is less important in synthetic cases. For the time-overcurrent relays, the model will protect the line from faults, but the relays are not coordinated. Proper zone 2 and zone 3 reach and load blinders as well as relay coordination are topics for future work.

The generator capability curves are accurate enough to be a better representation of the generator's reactive power capability than the capability "box" stored in the case. Future work on this topic could include using these equations that estimate the curve, to produce generator parameters. Currently, synthetic generator parameters are within an acceptable range; this algorithm could potentially be used as a tool to make the

parameters that are related to the generator capability curve more precise.

The methods presented in this study will allow researchers to improve their models so that their studies more accurately reflect the real grid. Achieving this in a purely synthetic model is important so that the results of the study can still be freely shared with other researchers.

REFERENCES

- [1] A. B. Birchfield, T. Xu, K. M. Gegner, K. S. Shetye, and T. J. Overbye, "Grid structural characteristics as validation criteria for synthetic networks," *IEEE Transactions on Power Systems*, vol. 32, no. 4, pp. 3258–3265, 2017, cite when using Adam's synthetic systems. [Online]. Available: <https://dx.doi.org/10.1109/TPWRS.2016.2616385>
- [2] T. Xu, A. B. Birchfield, K. M. Gegner, K. S. Shetye, and T. J. Overbye, "Application of large-scale synthetic power system models for energy economic studies," in *Proceedings of the 50th Hawaii International Conference on System Sciences*, 2017, Conference Proceedings.
- [3] T. J. Overbye, J. Snodgrass, A. Birchfield, and M. Stevens, "Towards developing implementable high altitude electromagnetic pulse e3 mitigation strategies for large-scale electric grids." IEEE, 2022, Conference Proceedings. [Online]. Available: <https://dx.doi.org/10.1109/tpec54980.2022.9750778>
- [4] T. J. Overbye, K. S. Shetye, T. R. Hutchins, Q. Qiu, and J. D. Weber, "Power grid sensitivity analysis of geomagnetically induced currents," *IEEE Transactions on Power Systems*, vol. 28, no. 4, pp. 4821–4828, 2013. [Online]. Available: <https://dx.doi.org/10.1109/tpwrs.2013.2274624>
- [5] P. S. Kundur and O. P. Malik, *Reactive Capability Limits*, second edition. ed. New York: McGraw-Hill Education, 2022.
- [6] M. G. Lauby and E. Rollison, "Effects of geomagnetic disturbances on the North American bulk power system," 2012.
- [7] D. Esmail Moghadam, A. Shiri, S. Sadr, and D. A. Khaburi, "A practical method for calculation of over-excited region in the synchronous generator capability curves." IEEE, 2014, Conference Proceedings. [Online]. Available: <https://dx.doi.org/10.1109/isie.2014.6864702>
- [8] S. B. Farnham and R. W. Swarthout, "Field excitation in relation to machine and system operation [includes discussion]," *Transactions of the American Institute of Electrical Engineers. Part III: Power Apparatus and Systems*, vol. 72, pp. 1215–1223, 1953.
- [9] I. G. Fernandes, V. L. Paucar, and O. R. Saavedra, "Optimal power flow solution including the synchronous generator capability curve constraints with a convex relaxation method." IEEE, 2017, Conference Proceedings. [Online]. Available: <https://dx.doi.org/10.1109/urucon.2017.8171891>
- [10] B. Tamimi, C. A. Canizares, and S. Vaez-Zadeh, "Effect of reactive power limit modeling on maximum system loading and active and reactive power markets," *IEEE Transactions on Power Systems*, vol. 25, no. 2, pp. 1106–1116, 2010. [Online]. Available: <https://dx.doi.org/10.1109/tpwrs.2009.2036798>
- [11] D. K. Molzahn, Z. B. Friedman, B. C. Lesieutre, C. L. Demarco, and M. C. Ferris, "Estimation of constraint parameters in optimal power flow data sets." IEEE, 2015, Conference Proceedings. [Online]. Available: <https://dx.doi.org/10.1109/naps.2015.7335092>
- [12] K. Yamashita, L. Juan, P. Zhang, and C.-C. Liu, "Analysis and control of major blackout events." IEEE, 2009, Conference Proceedings. [Online]. Available: <https://dx.doi.org/10.1109/psce.2009.4840091>
- [13] "Electric grid test case repository." Texas A&M University. [Online]. Available: <https://electricgrids.engr.tamu.edu/>
- [14] A. B. Birchfield, T. J. Overbye, and K. R. Davis, "Educational applications of large synthetic power grids," *IEEE Transactions on Power Systems*, vol. 34, no. 1, pp. 765–772, 2019. [Online]. Available: <https://dx.doi.org/10.1109/tpwrs.2018.2859910>
- [15] J. L. Blackburn and T. J. Domin, "Protective relaying," 2006. [Online]. Available: <https://dx.doi.org/10.1201/9781420017847>
- [16] V. Gurevich, "Electric relays," 2016. [Online]. Available: <https://dx.doi.org/10.1201/9781315221168>
- [17] P. M. Anderson, C. Henville, R. Rifaat, B. Johnson, and S. Meliopoulos, *Power system protection*. John Wiley & Sons, 2022.
- [18] E. O. Schweitzer and S. E. Zocholl, "The universal overcurrent relay," *IEEE Industry Applications Magazine*, vol. 2, no. 3, pp. 28–34, 1996. [Online]. Available: <https://dx.doi.org/10.1109/2943.491383>